PERGAMON

International Journal of Hydrogen Energy 25 (2000) 919–943

International Journal of HYDROGEN ENERGY

www.elsevier.com/locate/ijhydene

Observation of extreme ultraviolet hydrogen emission from incandescently heated hydrogen gas with certain catalysts

Randell L. Mills*, Jinquan Dong, Ying Lu

BlackLight Power, Inc., 493 Old Trenton Road, Cranbury, NJ 08512, USA

Abstract

Typically the emission of extreme ultraviolet light from hydrogen gas is achieved via a discharge at high voltage, a high power inductively coupled plasma, or a plasma created and heated to extreme temperatures by RF coupling (e.g. $> 10^6$ K) with confinement provided by a toroidal magnetic field. We report the observation of intense extreme ultraviolet (EUV) emission at low temperatures (e.g. $< 10^3$ K) from atomic hydrogen and certain atomized pure elements or certain gaseous ions which ionize at integer multiples of the potential energy of atomic hydrogen.

1. Introduction

A historical motivation to cause extreme ultraviolet (EUV) emission from a hydrogen gas was that the spectrum of hydrogen was first recorded from the only known source, the Sun [1]. Developed sources that provide a suitable intensity are high voltage discharge, synchrotron, and inductively coupled plasma generators [2]. An important variant of the latter type of source is a tokomak [3]. Fujimoto et al. [4] have determined the cross section for production of excited hydrogen atoms from the emission cross sections for Lyman and Balmer lines when molecular hydrogen is dissociated into excited atoms by electron collisions. This data was used to develop a collisional-radiative model to be used in determining the ratio of molecular-to-atomic hydrogen densities in tokomak plasmas. Their results indicate an excitation threshold of 17 eV for Lyman α emission. Addition of other gases would be expected to decrease the intensity of hydrogen lines which could be absorbed by the gas. Hollander and Wertheimer [5] found that within a selected range of parameters of a plasma created in a microwave resonator cavity, a hydrogen–oxygen plasma displays an emission that resembles the absorption of molecular oxygen. Whereas, a helium–hydrogen plasma emits a very intense hydrogen Lyman α radiation at 121.5 nm which is up to 40 times more intense than other lines in the spectrum. The Lyman α emission intensity showed a significant deviation from that predicted by the model of Fujimoto et al. [4] and from the emission of hydrogen alone.

We report that EUV emission of atomic and molecular hydrogen occurs in the gas phase at low temperatures (e.g. $< 10^3$ K) upon contact of atomic hydrogen with certain vaporized elements or ions. Atomic hydrogen was generated by dissociation at a tungsten filament and at a transition metal dissociator that was incandescently heated by the filament. Various elements or ions were atomized by heating to form a low vapor pressure (e.g. 1 torr). The kinetic

* Corresponding author. Tel.: +1-609-490-1090; fax: +1-609-490-1066.

E-mail address: rmills@blacklightpower.com (R.L. Mills).

0360-3199/00/$20.00
PII: S0360-3199(00)00018-5

energy of the thermal electrons at the experimental temperature of $<10^3$ K was about 0.1 eV, and the average collisional energies of electrons accelerated by the field of the filament were less than 1 eV. (No blackbody emission was recorded for wavelengths shorter than 400 nm.) Atoms or ions which ionize at integer multiples of the potential energy of atomic hydrogen (e.g. cesium, potassium, strontium, and Rb^+) caused emission; whereas, other chemically equivalent or similar atoms (e.g. sodium, magnesium, holmium, and zinc metals) caused no emission. Helium ions present in the experiment of Hollander and Wertheimer [5] ionize at a multiple of two times the potential energy of atomic hydrogen. The mechanism of EUV emission cannot be explained by the conventional chemistry of hydrogen, but it is predicted by a solution of the Schrodinger equation with a nonradiative boundary constraint put forward by Mills [6].

Mills predicts that certain atoms or ions serve as catalysts to release energy from hydrogen to produce an increased binding energy hydrogen atom called a *hydrino atom* having a binding energy of

$$\text{Binding energy} = \frac{13.6\,\text{eV}}{n^2} \tag{1}$$

where

$$n = \frac{1}{2}, \frac{1}{3}, \frac{1}{4}, \ldots, \frac{1}{p} \tag{2}$$

and p is an integer greater than 1, designated as $H[\frac{a_H}{p}]$ where a_H is the radius of the hydrogen atom. Hydrinos are predicted to form by reacting an ordinary hydrogen atom with a catalyst having a net enthalpy of reaction of about

$$m \cdot 27.2\,\text{eV} \tag{3}$$

where m is an integer. This catalysis releases energy from the hydrogen atom with a commensurate decrease in size of the hydrogen atom, $r_n = na_H$. For example, the catalysis of $H(n = 1)$ to $H(n = 1/2)$ releases 40.8 eV, and the hydrogen radius decreases from a_H to $\frac{1}{2}a_H$.

The excited energy states of atomic hydrogen are also given by Eq. (1) except that

$$n = 1, 2, 3, \ldots \tag{4}$$

The $n = 1$ state is the 'ground' state for 'pure' photon transitions (the $n = 1$ state can absorb a photon and go to an excited electronic state, but it cannot release a photon and go to a lower-energy electronic state). However, an electron transition from the ground state to a lower-energy state is possible by a nonradiative energy transfer such as multipole coupling or a resonant collision mechanism. These lower-energy states have fractional quantum numbers, $n = \frac{1}{\text{integer}}$. Processes that occur without photons and that require collisions are common. For example, the exothermic chemical reaction of H + H to form H_2 does not occur with the emission of a photon. Rather, the reaction requires a collision with a third body, M, to remove the bond energy — $H + H + M \rightarrow H_2 + M^*$ [7]. The third body distributes the energy from the exothermic reaction, and the end result is the H_2 molecule and an increase in the temperature of the system. Some commercial phosphors are based on nonradiative energy transfer involving multipole coupling. For example, the strong absorption strength of Sb^{3+} ions along with the efficient nonradiative transfer of excitation from Sb^{3+} to Mn^{2+}, are responsible for the strong manganese luminescence from phosphors containing these ions. Similarly, the $n = 1$ state of hydrogen and the $n = \frac{1}{\text{integer}}$ states of hydrogen are nonradiative, but a transition between two nonradiative states is possible via a nonradiative energy transfer, say $n = 1$ to $n = 1/2$. In these cases, during the transition the electron couples to another electron transition, electron transfer reaction, or inelastic scattering reaction which can absorb the exact amount of energy that must be removed from the hydrogen atom. Thus, a catalyst provides a net positive enthalpy of reaction of $m \cdot 27.2$ eV (i.e. it absorbs $m \cdot 27.2$ eV where m is an integer). Certain atoms or ions serve as catalysts which resonantly accept energy from hydrogen atoms and release the energy to the surroundings to effect electronic transitions to fractional quantum energy levels.

An example of *nonradiative energy transfer* is the basis of commercial fluorescent lamps [8]. Consider Mn^{2+} which when excited sometimes emits yellow luminescence. The absorption transitions of Mn^{2+} are spin-forbidden. Thus, the absorption bands are weak, and the Mn^{2+} ions cannot be efficiently raised to excited states by direct optical pumping. Nevertheless, Mn^{2+} is one of the most important luminescence centers in commercial phosphors. For example, the double-doped phosphor $Ca_5(PO_4)_3$ F: Sb^{3+}, Mn^{2+} is used in commercial fluorescent lamps where it converts mainly ultraviolet light from a mercury discharge into visible radiation. When 2536 Å mercury radiation falls on this material, the radiation is absorbed by the Sb^{3+} ions rather than the Mn^{2+} ions. Some excited Sb^{3+} ions emit their characteristic blue luminescence, while other excited Sb^{3+} ions transfer their energy to Mn^{2+} ions. These excited Mn^{2+} ions emit their characteristic yellow luminescence. The efficiency of transfer of ultraviolet photons through the Sb^{3+} ions to the Mn^{2+} ions can be as high as 80%. The strong absorption strength of Sb^{3+} ions along with the efficient transfer of excitation from Sb^{3+} to Mn^{2+} are responsible for the strong manganese luminescence from this material.

This type of *nonradiative energy transfer* is common.

The ion which emits the light and which is the active element in the material is called the activator; and the ion which helps to excite the *activator* and makes the material more sensitive to pumping light is called the *sensitizer*. Thus, the sensitizer ion absorbs the radiation and becomes excited. Because of a coupling between sensitizer and activator ions, the sensitizer transmits its excitation to the activator, which becomes excited, and the activator may release the energy as its own characteristic radiation. The sensitizer to activator transfer is

Table 1
Hydrogen catalysts providing a net positive enthalpy of reaction of m·27.2 eV by one or more electron ionizations to the continuum level

Catalysts	IP_1	IP_2	IP_3	IP_4	IP_5	IP_6	IP_7	IP_8	Enthalpy	m
Li	5.39172	75.6402							81.032	3
Be	9.32263	18.2112							27.534	1
B	4.34066	31.63	45.806						81.777	3
Na	6.11316	11.8717	50.9131	67.27					136.17	5
Mg	6.8282	13.5755	27.4917	43.267	99.3				190.46	7
Al	6.7463	14.66	29.311	46.709	65.2817				162.71	6
Ar	6.76664	16.4857	30.96						54.212	2
In	7.43402	15.64	33.668	51.2					107.94	4
Se	7.9024	16.1878	30.652						54.742	2
Se	7.9024	16.1878	30.652	54.8					109.54	4
Co	7.881	17.083	33.5	51.3					109.76	4
Co	7.881	17.083	33.5	51.3	79.5				189.26	7
Ni	7.6398	18.1688	35.19	54.9	76.06				191.96	7
Ni	7.6398	18.1688	35.19	54.9	76.06	108			299.96	11
Cu	7.72638	20.2924							28.019	1
Zn	9.39405	17.9644							27.358	1
Zn	9.39405	17.9644	39.723	59.4	82.6	108	134	174	625.08	23
Ga	9.8152	18.633	28.351	50.13	62.63	127.6			297.16	11
	9.75238	21.19	30.8204	42.945	68.3	81.7	155.4		410.11	15
Kr	13.9996	24.3599	36.95	52.5	64.7	78.5			271.01	10
Kr	13.9996	24.3599	36.95	52.5	64.7	78.5	111		382.01	14
Rb	4.17713	27.285	40	52.6	71	84.4	99.2		378.66	14
Rb	4.17713	27.285	40	52.6	71	84.4	99.2	136	514.66	19
	5.69484	11.0301	42.89	57	71.6				188.21	7
Sr	6.75885	14.32	25.04	38.3	50.55				134.97	5
Mo	7.09243	16.16	27.13	46.4	54.49	68.8276			151.27	8
Mo	7.09243	16.16	27.13	46.4	54.49	68.8276	125.664	143.6	489.36	18
	8.3369	19.43							27.767	1
	7.34381	14.6323	30.5026	40.735	72.28				165.49	6
	9.0096	18.6							27.61	1
	9.0096	18.6	27.96						55.57	2
	3.8939	23.1575							27.051	1
	5.5387	10.85	20.198	36.758	65.55				138.89	5
	5.5387	10.85	20.198	36.758	65.55	77.6			216.49	8
	5.464	10.55	21.624	38.98	57.53				134.15	5
	5.6437	11.07	23.4	41.4					81.514	3
	6.15	12.09	20.63	44					82.87	3
	5.9389	11.67	22.8	41.47					81.879	3
	7.41666	15.0322	31.9373						54.386	2
	8.9587	18.563							27.522	1
+		54.4178							54.418	2
+		47.2864	71.6200	98.91					217.816	8
+		27.285							27.285	1
+				54.8					54.8	2
2+			27.13						27.13	1
4+					54.49				54.49	2
+				54					54	2

not a radiative emission and absorption process, rather a *nonradiative transfer*. The nonradiative transfer may be by electric or magnetic multipole interactions. In the transfer of energy between dissimilar ions, the levels will, in general, not be in resonance, and some of the energy is released as a phonon or phonons. In the case of similar ions, the levels should be in resonance, and phonons are not needed to conserve energy.

Sometimes the host material itself may absorb (usually in the ultraviolet) and the energy can be transferred nonradiatively to dopant ions. For example, in YVO_4: Eu^{3+}, the vanadate group of the host material absorbs ultraviolet light, then transfers its energy to the Eu^{3+} ions which emit characteristic Eu^{3+} luminescence.

The catalysis of hydrogen involves the nonradiative transfer of energy from atomic hydrogen to a catalyst which may then release the transferred energy by radiative and nonradiative mechanisms. As a consequence of the nonradiative energy transfer, the hydrogen atom becomes unstable and emits further energy until it achieves a lower-energy nonradiative state having a principal energy level given by Eq. (1).

For example, a catalytic system is provided by the ionization of t electrons from an atom each to a continuum energy level such that the sum of the ionization energies of the t electrons is approximately $m \cdot 27.2$ eV where t and m are each an integer. One such catalytic system involves cesium. The first and second ionization energies of cesium are 3.89390 eV and 23.15745 eV, respectively [9]. The double ionization ($t = 2$) reaction of Cs to Cs^{2+}, then, has a net enthalpy of reaction of 27.05135 eV, which is equivalent to $m = 1$ in Eq. (3).

$$27.05135\,\text{eV} + \text{Cs}(m) + \text{H}\left[\frac{a_H}{p}\right] \rightarrow \text{Cs}^{2+} + 2e^- + \text{H}\left[\frac{a_H}{(p+1)}\right] + [(p+1)^2 - p^2] \times 13.6\,\text{eV} \quad (5)$$

$$\text{Cs}^{2+} + 2e^- \rightarrow \text{Cs}(m) + 27.05135\,\text{eV} \quad (6)$$

And, the overall reaction is

$$H\left[\frac{a_H}{p}\right] \rightarrow \text{H}\left[\frac{a_H}{(p+1)}\right] + [(p+1)^2 - p^2] \times 13.6\,\text{eV} \quad (7)$$

Thermal energies may broaden the enthalpy of reaction. The relationship between kinetic energy and temperature is given by

$$E_{\text{kinetic}} = \frac{3}{2}kT \quad (8)$$

For a temperature of 1200 K, the thermal energy is 0.16 eV, and the net enthalpy of reaction provided by cesium metal is 27.21 eV which is an exact match to the desired energy.

Hydrogen catalysts capable of providing a net enthalpy of reaction of approximately $m \cdot 27.2$ eV where m is an integer to produce hydrino whereby t electrons are ionized from an atom or ion are given in Table 1. The atoms or ions given in the first column are ionized to provide the net enthalpy of reaction of $m \cdot 27.2$ eV given in the tenth column where m is given in the eleventh column. The electrons which are ionized are given with the ionization potential (also called ionization energy or binding energy). The ionization potential of the nth electron of the atom or ion is designated by IP_n and is given by the CRC [9]. That is, for example, $Cs + 3.89390\,\text{eV} \rightarrow Cs^+ + e^-$ and $Cs^+ + 23.15745\,\text{eV} \rightarrow Cs^{2+} + e^-$. The first ionization potential, $IP_1 = 3.89390$ eV, and the second ionization potential, $IP_2 = 23.15745$ eV, are given in the second and third columns, respectively. The net enthalpy of reaction for the double ionization of Cs is 27.05135 eV as given in the tenth column, and $m = 1$ in Eq. (3) as given in the eleventh column.

The energy released during catalysis may undergo internal conversion and ionize or excite molecular and atomic hydrogen resulting in hydrogen emission which includes well characterized ultraviolet lines such as the Lyman series. Lyman α emission was sought by EUV spectroscopy. Due to the extremely short wavelength of this radiation, 'transparent' optics do not exist. Therefore, a windowless arrangement was used wherein the source was connected to the same vacuum vessel as the grating and detectors of the EUV spectrometer. Windowless EUV spectroscopy was performed with an extreme ultraviolet spectrometer that was mated with the cell. Differential pumping permitted a high pressure in the cell as compared to that in the spectrometer. This was achieved by pumping on the cell outlet and pumping on the grating side of the collimator that served as a pin-hole inlet to the optics. The cell was operated under hydrogen flow conditions while maintaining a constant hydrogen pressure in the cell with a mass flow controller.

2. Experimental

The experimental set up, shown in Fig. 1, comprised a quartz cell which was 500 mm in length and 50 mm in diameter. A sample reservoir that was heated independently using an external heater powered by a constant power supply was on one end of the quartz cell. Three ports for gas inlet, outlet, and photon detection were on the other end of the cell. A tungsten filament (0.5 mm, total resistance ~2.5 ohm) and a titanium or nickel cylindrical screen (300 mm long and 40 mm in diameter) that performed as a hydrogen dissociator

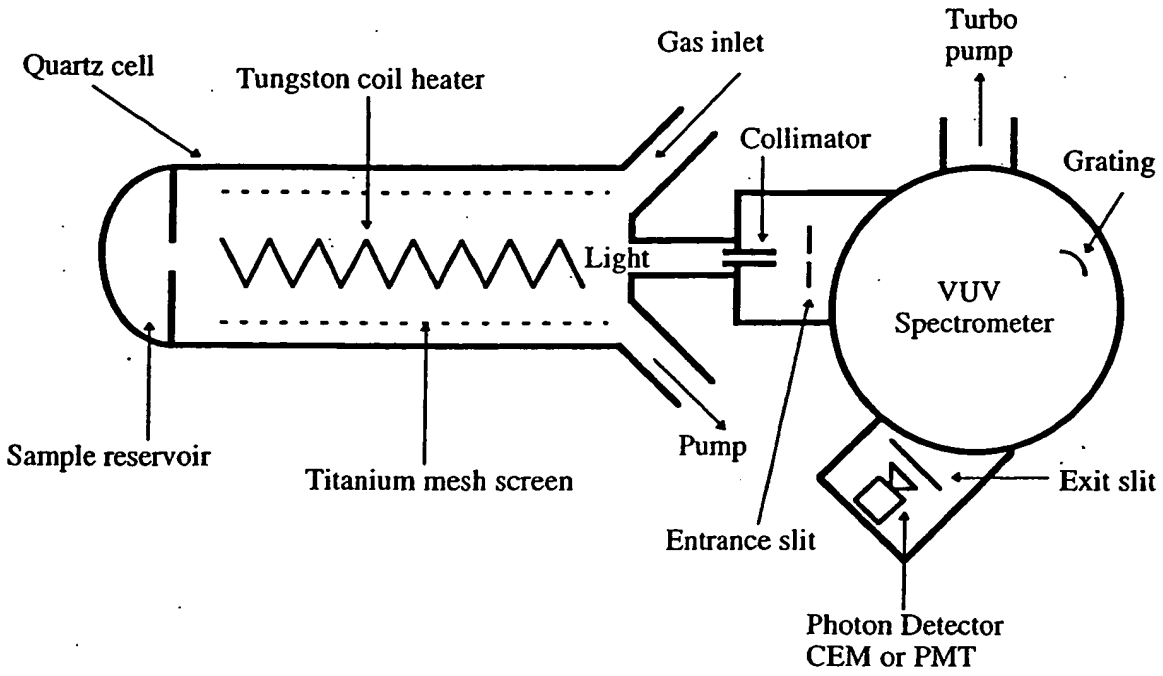

Fig. 1. The experimental set up comprising a gas cell light source and an EUV spectrometer which was differentially pumped.

were inside the quartz cell. The filament was 0.508 mm in diameter and 800 cm in length. The filament was coiled on a grooved ceramic support to maintain its shape when heated. The return lead ran through the middle of the ceramic support. The titanium screen was electrically floated. The power applied to the filament ranged from 300 to 600 W and was supplied by a Sorensen 80–13 power supply which was controlled by a constant power controller. The voltage across the filament was about 55 V and the current was about 5.5 A at 300 W. The temperature of the tungsten filament was estimated to be in the range of 1100 to 1500°C. The external cell wall temperature was about 700°C. The hydrogen gas pressure inside the cell was maintained at about 300 mtorr. The entire quartz cell was enclosed inside an insulation package comprised of Zircar AL-30 insulation. Several K type thermocouples were placed in the insulation to measure key temperatures of the cell and insulation. The thermocouples were read with a multichannel computer data acquisition system.

In the present study, the light emission phenomena was studied for more than 130 inorganic compounds and pure elements. The inorganic test materials were coated on a titanium or nickel screen dissociator by the method of incipient wetness. That is the screen was coated by dipping it in a concentrated deionized aqueous solution or suspension, and the crystalline material was dried on the surface by heating for 12 h in a drying oven at 130°C. A new dissociator was used for each experiment. The chemicals on the screen were heated by the tungsten filament and vaporized. Pure elements with a high vapor pressure as well as inorganic compounds were placed in the reservoir and volatized by the external heater. Test chemicals with a low vapor pressure (high melting point) were volatilized by suspending a foil of the material (2 cm by 2 cm by 0.1 cm thick) between the filament and a titanium or nickel dissociator and heating the test material with the filament. The cell was increased in temperature to the maximum possible that was permissible with the power supply (about 300 W).

The light emission was introduced to a EUV spectrometer for spectral measurement. The spectrometer was a McPherson 0.2 m monochromator (Model 302, Seya-Namioka type) equipped with a 1200 lines/mm holographic grating. The wavelength region covered by the monochromator was 30–560 nm. A channel electron multiplier (CEM) was used to detect the EUV light. The wavelength resolution was about 12 nm (FWHM) with an entrance and exit slit width of 300 × 300 μm. The vacuum inside the monochromator was maintained below 5×10^{-4} torr by a turbo pump. The EUV spectrum (40–160 nm) of the cell emission was recorded at about the point of the maximum Lyman α emission.

In the case that a hazardous test material was run, the cell was closed, and the UV–VIS spectrum (300–560 nm) of the cell emission was recorded with a photomultiplier tube (PMT) and a sodium salicylate scintillator. The PMT (model R1527P, Hamamatsu) used has a spectral response in the range of 185–680 nm with a peak efficiency at about 400 nm. The scan interval was 0.4 nm. The inlet and outlet slit were 500–500 μm.

The UV–VIS emission from the gas cell was channeled into the UV–VIS spectrometer using a 4 m long, five stand fiber optic cable (Edmund Scientific Model #E2549) having a core diameter of 1958 μm and a maximum attenuation of 0.19 dB/m. The fiber optic cable was placed on the outside surface of the top of the Pyrex cap of the gas cell. The fiber was oriented to maximize the collection of light emitted from inside the cell. The room was made dark. The other end of the fiber optic cable was fixed in a aperture manifold that attached to the entrance aperture of the UV–VIS spectrometer.

The experiments performed according to number were:

1. KCl/10% H_2O_2 treated titanium dissociator with tungsten filament
2. K_2CO_3/10% H_2O_2 treated titanium dissociator with tungsten filament and RbCl in the catalyst reservoir
3. K_2CO_3/10% H_2O_2 treated titanium dissociator with tungsten filament
4. Na_2CO_3/10% H_2O_2 treated titanium dissociator with tungsten filament
5. Rb_2CO_3/10% H_2O_2 treated titanium dissociator with tungsten filament
6. Cs_2CO_3/10% H_2O_2 treated titanium dissociator with tungsten filament
7. repeat Na_2CO_3/10% H_2O_2 treated titanium dissociator with tungsten filament
8. K_2CO_3 /10% H_2O_2 treated nickel dissociator with tungsten filament
9. KNO_3/10% H_2O_2 treated titanium dissociator with tungsten filament
10. repeat K_2CO_3/10% H_2O_2 treated titanium dissociator with tungsten filament
11. K_2SO_4/10% H_2O_2 treated titanium dissociator with tungsten filament
12. $LiNO_3$/10% H_2O_2 treated titanium dissociator with tungsten filament
13. Li_2CO_3/10% H_2O_2 treated titanium dissociator with tungsten filament
14. $MgCO_3$/10% H_2O_2 treated titanium dissociator with tungsten filament
15. repeat RbCl/10% H_2O_2 treated titanium dissociator with tungsten filament; run at very high temperature to volatilize the catalyst
16. RbCl/10% H_2O_2 treated titanium dissociator with tungsten filament and RbCl in the catalyst reservoir
17. K_2CO_3 coated on titanium dissociator with tungsten filament
18. $KHCO_3$/10% H_2O_2 treated titanium dissociator with tungsten filament
19. $CaCO_3$/10% H_2O_2 treated titanium dissociator with tungsten filament
20. K_3PO_4/10% H_2O_2 treated titanium dissociator with tungsten filament
21. samarium foil with titanium dissociator and tungsten filament
22. zinc foil with titanium dissociator and tungsten filament
23. iron foil with titanium dissociator and tungsten filament
24. copper foil with titanium dissociator and tungsten filament
25. chromium foil with titanium dissociator and tungsten filament
26. holmium foil with titanium dissociator and tungsten filament
27. potassium metal in catalyst reservoir with titanium dissociator and tungsten filament
28. dysprosium foil with titanium dissociator and tungsten filament
29. magnesium foil with titanium dissociator and tungsten filament
30. sodium metal in catalyst reservoir with titanium dissociator and tungsten filament
31. rubidium metal in catalyst reservoir with titanium dissociator and tungsten filament
32. cobalt foil with titanium dissociator and tungsten filament
33. lead foil with titanium dissociator and tungsten filament; used closed cell with Balmer line detection by fiber optic cable as indication of EUV
34. manganese foil with titanium dissociator and tungsten filament
35. gadolinium foil with titanium dissociator and tungsten filament
36. lithium metal in catalyst reservoir with titanium dissociator and tungsten filament
37. praseodymium foil with titanium dissociator and tungsten filament
38. vanadium foil with titanium dissociator and tungsten filament
39. tin foil with titanium dissociator and tungsten filament
40. platinum foil with titanium dissociator and tungsten filament
41. palladium foil with titanium dissociator and tungsten filament
42. erbium foil with titanium dissociator and tungsten filament
43. aluminum foil with titanium dissociator and tung-

sten filament
44. nickel foil with titanium dissociator and tungsten filament
45. molybdenum foil with titanium dissociator and tungsten filament
46. cerium foil with titanium dissociator and tungsten filament
47. repeat potassium metal in catalyst reservoir with titanium dissociator and tungsten filament at lower catalyst reservoir heater power to keep potassium metal in reaction zone longer
48. niobium foil with titanium dissociator and tungsten filament
49. tungsten filament with titanium dissociator and mixture of potassium metal and rubidium metal
50. repeat cobalt foil with titanium dissociator and tungsten filament
51. silver foil with titanium dissociator and tungsten filament
52. calcium metal in catalyst reservoir with titanium dissociator and tungsten filament
53. chromium foil with titanium dissociator and tungsten filament
54. K_2CO_3 coated on nickel dissociator and tungsten filament
55. $KHSO_4$ coated titanium dissociator and tungsten filament
56. $KHCO_3$ coated titanium dissociator and tungsten filament
57. cesium metal in catalyst reservoir with titanium dissociator and tungsten filament
58. neon gas with titanium dissociator and tungsten filament
59. MoI_2 in catalyst reservoir with titanium dissociator and tungsten filament at low catalyst reservoir heater power to keep MoI_2 in reaction zone
60. repeat Cs_2CO_3 coated titanium dissociator and tungsten filament
61. osmium foil with titanium dissociator and tungsten filament
62. high purity carbon rod with titanium dissociator and tungsten filament
63. repeat lithium metal in catalyst reservoir with titanium dissociator and tungsten filament
64. tantalum foil with titanium dissociator and tungsten filament
65. KH_2PO_4/10% H_2O_2 treated titanium dissociator and tungsten filament
66. etched germanium with titanium dissociator and tungsten filament
67. helium gas with titanium dissociator and tungsten filament
68. etched silicon with titanium dissociator and tungsten filament
69. bismuth foil in catalyst reservoir with titanium dissociator and tungsten filament
70. Strontium metal in catalyst reservoir with titanium dissociator and tungsten filament
71. etched gallium in catalyst reservoir with titanium dissociator and tungsten filament
72. repeat iron foil with titanium dissociator and tungsten filament
73. argon gas with titanium dissociator and tungsten filament
74. selenium foil in catalyst reservoir with titanium dissociator and tungsten filament; used closed cell with Balmer line detection by fiber optic cable as indication of EUV
75. RbI + KI coated titanium dissociator with tungsten filament
76. $SrCl_2$ + $FeCl_2$ coated titanium dissociator with tungsten filament
77. indium foil with titanium dissociator and tungsten filament
78. zirconium foil with titanium dissociator and tungsten filament
79. barium metal in catalyst reservoir with titanium dissociator and tungsten filament
80. antimony foil in catalyst reservoir with titanium dissociator and tungsten filament
81. ruthenium foil with titanium dissociator and tungsten filament
82. yttrium foil in catalyst reservoir with titanium dissociator and tungsten filament
83. cadmium foil with titanium dissociator and tungsten filament
84. repeat samarium foil with titanium dissociator and tungsten filament
85. K_2HPO_4 coated titanium dissociator with tungsten filament
86. $SrCO_3$ coated titanium dissociator with tungsten filament
87. $ErCl_3$ + $MgCl_2$ coated titanium dissociator with tungsten filament
88. LiF + $PdCl_2$ coated titanium dissociator with tungsten filament
89. $EuCl_3$ + $MgCl_2$ coated titanium dissociator with tungsten filament
90. La_2 $(CO_3)_3$ coated titanium dissociator with tungsten filament
91. Ag_2SO_4 coated titanium dissociator with tungsten filament
92. $Er_2(CO_3)_3$ coated titanium dissociator with tungsten filament
93. repeat samarium foil third time with titanium dissociator and tungsten filament
94. $Y_2(SO_4)_3$ coated titanium dissociator with tungsten filament
95. SiO_2 coated titanium dissociator with tungsten filament
96. $Zn(NO_3)_2$ coated titanium dissociator with tungsten filament

Table 2
Extreme ultraviolet light emission from atomic hydrogen and atomized pure elements or gaseous inorganic compounds at low temperatures (e.g. $< 10^3$ K)

Element[a]	Compound[a]	Experiment number	Gas	Condensed metal vapor coating observed	Maximum intensity at zero order (counts/s)	Maximum intensity of hydrogen lyman α (counts/sec)[b]
	KCl/H_2O_2	1	H_2		Presence of blue light by eye	
	K_2CO_3/H_2O_2 and RbCl in reservoir	2	H_2	Yes	Balmer β 300	
	K_2CO_3/H_2O_2	3	H_2	Yes		60000
	Na_2CO_3/H_2O_2	4	H_2	Yes		–
	Rb_2CO_3/H_2O_2	5	H_2	Yes		20000
	Cs_2CO_3/H_2O_2	6	H_2	Yes		30000
	Na_2CO_3/H_2O_2	7	H_2	Yes		–
	K_2CO_3/H_2O_2 nickel dissociator	8	H_2	Yes		10000
	KNO_3/H_2O_2	9	H_2	Yes		25000
	K_2CO_3/H_2O_2	10	H_2	Yes		30000
	K_2SO_4/H_2O_2	11	H_2	Yes		2000
	$LiNO_3/H_2O_2$	12	H_2	No		5000
	Li_2CO_3/H_2O_2	13	H_2	No		2500
	$MgCO_3/H_2O_2$	14	H_2	No		150
	$RbCl/H_2O_2$	15	H_2	No		–
	$RbCl/H_2O_2$ and RbCl in reservoir	16	H_2	Yes		–
	K_2CO_3	17	H_2	Yes		2000
	$KHCO_3/H_2O_2$	18	H_2	Yes		40000
	$CaCO_3/H_2O_2$	19	H_2	Yes		2500
	K_3PO_4/H_2O_2	20	H_2	Yes		7000
Samarium		21	H_2	Yes		3000
Zinc		22	H_2	Yes		–
Iron		23	H_2	No		11000
Copper		24	H_2	No		–
Chromium		25	H_2	No		–
Holmium		26	H_2	No		100
Potassium metal in reservoir		27	H_2	Yes		6000
Dysprosium		28	H_2	No	–	
Magnesium		29	H_2	Yes	–	
Sodium metal in reservoir		30	H_2	Yes		170
Rubidium metal in reservoir		31	H_2	Yes		12000
Cobalt		32	H_2	No		–
Lead		33	H_2	Yes	Balmer β	–
Manganese		34	H_2	Yes		–
Gadolinium		35	H_2	No		–
Lithium metal in reservoir[c]		36	H_2			
Praseodymium		37	H_2	No		2500

Tin		39	H_2	No		–
Platinum		40	H_2	No		–
Palladium		41	H_2	No		–
Erbium		42	H_2	No		–
Aluminum		43	H_2	No		–
Nickel		44	H_2	No		–
Molybdenum		45	H_2	No		–
Cerium		46	H_2	No		–
Potassium metal in reservoir		47	H_2	Yes		8700
Niobium		48	H_2	No		–
Potassium and rubidium metals in reservoir		49	H_2	Yes		12000
Cobalt		50	H_2	No		–
Silver		51	H_2	No		–
Calcium metal in reservoir		52	H_2	Yes		16000
Chromium		53	H_2	No		–
	K_2CO_3[d]nickel dissociator	54	H_2	Yes		300
	$KHSO_4$	55	H_2	Yes		–
	$KHCO_3$	56	H_2	Yes		3000
Cesium metal in reservoir		57	H_2	Yes		60000
Neon gas		58	H_2	No		–
	MoI_2 in reservoir	59	H_2	Yes		–
	Cs_2CO_3	60	H_2	Yes		40000
Osmium		61	H_2	No		–
Carbon		62	H_2	No		–
Lithium metal in reservoir		63	H_2	Yes		200
Tantalum		64	H_2	No		–
	KH_2PO_4/H_2O_2	65	H_2	Yes		100
Germanium		66	H_2	No		–
Helium gas		67	He	No		–
Silicon		68	H_2	No		–
Bismuth		69	H_2	No		–
Strontium metal in reservoir		70	H_2	Yes		39000
Gallium in reservoir		71	H_2	No		–
Iron		72	H_2	No		800
Argon gas		73	H_2	No		–
Selenium		74	H_2	No	Balmer β	
	RbI + KI	75	H_2	No		200
	$SrCl_2$ + $FeCl_2$[e]	76	H_2	No		–
Indium		77	H_2	No		–
Zirconium		78	H_2	No		–
Barium metal in reservoir		79	H_2	No		–
Antimony in reservoir		80	H_2	No		–
Ruthenium		81	H_2	No		140

(continued on next page)

Table 2 (*continued*)

Element[a]	Compound[a]	Experiment number	Gas	Condensed metal vapor coating observed	Maximum intensity at zero order (counts/s)	Maximum intensity of hydrogen lyman α (counts/sec)[b]
Yttrium metal in reservoir		82	H_2	No		–
Cadmium		83	H_2	Yes		–
Samarium		84	H_2	Yes		200
	K_2HPO_4	85	H_2	Yes		4000
	$SrCO_3$	86	H_2	Yes		39000
	$ErCl_3 + MgCl_2$	87	H_2	Yes		–
	$LiF + PdCl_2$	88	H_2	No		–
	$EuCl_3 + MgCl_2$	89	H_2	Yes		–
	$La_2(CO_3)_3$	90	H_2	Yes		6000
	Ag_2SO_4	91	H_2	Yes		–
	$Er_2(CO_3)_3$	92	H_2	No		–
Samarium		93	H_2	Yes		3000
	$Y_2(SO_4)_3$	94	H_2	No		–
	SiO_2	95	H_2	No		–
	$Zn(NO_3)_2$	96	H_2	Yes		–
	$Ba(NO_3)_2$	97	H_2	No		400000
	Al_2O_3	98	H_2	No		100
	$CrPO_4$	99	H_2	No		–
	$NaNO_3$	100	H_2	Yes		60000
	$Bi(NO_3)_3$	101	H_2	Yes		–
	$Sc_2(CO_3)_3$	102	H_2	No		–
Europium		103	H_2	No		–
Rhenium		104	H_2	No		–
Lutetium		105	H_2	No		–
	$Mg(NO_3)_2$	106	H_2	Yes		–
	$Sr(NO_3)_2$	107	H_2	No		20000
Neodymium		108	H_2	Yes		3000
Ytterbium		109	H_2	Yes		–
	$NaNO_3$	110	Helium	Yes		
Thallium		111	H_2	Yes		100
	$RbNO_3$	112	H_2	Yes		79000
Lanthanum		113	H_2	No		–
	$Sm(NO_3)_3$	114	H_2	Yes		2000
Terbium		115	H_2	No		–
	$La(NO_3)_3$	116	H_2	No		–
Hafnium		117	H_2	No		–
	$NaClO_3$	118	H_2	No		–
	$NaNO_3$	119	H_2	Yes		2500

	$Sm_2(CO_3)_3$	120	H_2	Yes		2000
Scandium		121	H_2	No		–
	NbO_2	122	H_2	No		–
	$KClO_3$	123	H_2	Yes		–
	$BaCO_3$	124	H_2	No		5000
	$Yb(NO_3)_3$	125	H_2	No		–
Thulium		126	H_2	Yes		–
	$Yb_2(CO_3)_3$	127	H_2	No		–
	$RbClO_3$	128	H_2	Yes		–
	HfI_4	129	H_2	Yes	–	–
Rhodium		130	H_2	No	–	
Iridium		131	H_2	No	–	
Gold		132	H_2	No	–	
Ytterbium		133	H_2	No	–	
Hafnium		134	H_2	No	–	
Potassium metal in reservoir		135	Argon	Yes	–	
Potassium metal in reservoir		136	Neon	Yes	100	
	K_2CO_3	137	Argon	Yes	30	
	NaI	138	H_2	No		

[a] Titanium screen dissociator and tungsten filament except where indicated.

[b] Lyman α was recorded except for toxic compounds wherein a window was used, and the maximum intensity of Balmer β emission was recorded in (counts/sec) where indicated.

[c] Quartz cell failed due to reaction with lithium metal.

[d] Only a small amount of K_2CO_3 on the titanium screen dissociator.

[e] Channel electron multiplier failed due to reaction with volatized compounds.

97. $Ba(NO_3)_2$ coated titanium dissociator with tungsten filament
98. Al_2O_3 coated titanium dissociator with tungsten filament
99. $CrPO_4$ coated titanium dissociator with tungsten filament
100. $NaNO_3$ coated titanium dissociator with tungsten filament
101. $Bi(NO_3)_3$ coated titanium dissociator with tungsten filament
102. $Sc_2(CO_3)_3$ coated titanium dissociator with tungsten filament
103. europium foil with titanium dissociator and tungsten filament
104. rhenium foil with titanium dissociator and tungsten filament
105. lutenium foil with titanium dissociator and tungsten filament
106. $Mg(NO_3)_2$ coated titanium dissociator with tungsten filament
107. $Sr(NO_3)_2$ coated titanium dissociator with tungsten filament
108. neodymium foil with titanium dissociator and tungsten filament
109. ytterbium foil with titanium dissociator and tungsten filament
110. $NaNO_3$ coated titanium dissociator with tungsten filament and helium (no hydrogen control)
111. thallium foil with titanium dissociator and tungsten filament
112. $RbNO_3$ coated titanium dissociator with tungsten filament
113. lanthanum foil with titanium dissociator and tungsten filament
114. $Sm(NO_3)_3$, coated titanium dissociator with tungsten filament
115. terbium foil with titanium dissociator and tungsten filament
116. $La(NO_3)_3$ coated titanium dissociator with tungsten filament
117. hafnium foil with titanium dissociator and tungsten filament
118. $NaClO_3$ coated titanium dissociator with tungsten filament
119. repeat $NaNO_3$ coated titanium dissociator with tungsten filament
120. $Sm_2(CO_3)_3$ coated titanium dissociator with tungsten filament
121. scandium foil with titanium dissociator and tungsten filament
122. NbO_2 coated titanium dissociator with tungsten filament
123. $KClO_3$ coated titanium dissociator with tungsten filament
124. $BaCO_3$ coated titanium dissociator with tungsten filament
125. $Yb(NO_3)_3$ coated titanium dissociator with tungsten filament
126. thulium foil with titanium dissociator and tungsten filament
127. $Yb_2(CO_3)_3$ coated titanium dissociator with tungsten filament
128. $RbClO_3$ coated titanium dissociator with tungsten filament
129. HfI_4 coated titanium dissociator with tungsten filament
130. rhodium foil with titanium dissociator and tungsten filament
131. iridium foil with titanium dissociator and tungsten filament
132. gold foil with titanium dissociator and tungsten filament
133. repeat ytterbium foil with titanium dissociator and tungsten filament
134. repeat hafnium foil with titanium dissociator and tungsten filament
135. potassium metal in catalyst reservoir with tungsten filament, titanium dissociator, and neon (no hydrogen control)
136. potassium metal in catalyst reservoir with tungsten filament, titanium dissociator, and argon (no hydrogen control)
137. K_2CO_3 treated titanium foil with tungsten filament and argon (no hydrogen control)
138. NaI treated titanium foil with tungsten filament

3. Results

The results of the extreme ultraviolet (EUV) light emission from atomic hydrogen and atomized pure elements or gaseous inorganic compounds at low temperatures (e.g. $<10^3$ K) are summarized in Table 2. The EUV light emission measurements were performed on more than 100 elements and inorganic compounds comprising 138 experiments as given in the experimental section.

The cell without any test material present was run to establish the baseline of the spectrometer. The intensity of the Lyman α emission as a function of time from the gas cell comprising a tungsten filament, a titanium dissociator, and 0.3 torr hydrogen at a cell temperature of 700°C is shown in Fig. 2 (A). The UV–VIS spectrum (40–560 nm) of the cell emission from the gas cell comprising a tungsten filament, a titanium dissociator, and 0.3 torr hydrogen at a cell temperature of 700°C is shown in Fig. 2 (B). The spectrum was recorded with a photomultiplier tube (PMT) and a sodium salicylate scintillator. No emission was observed except for the blackbody filament radiation at the longer wavelengths.

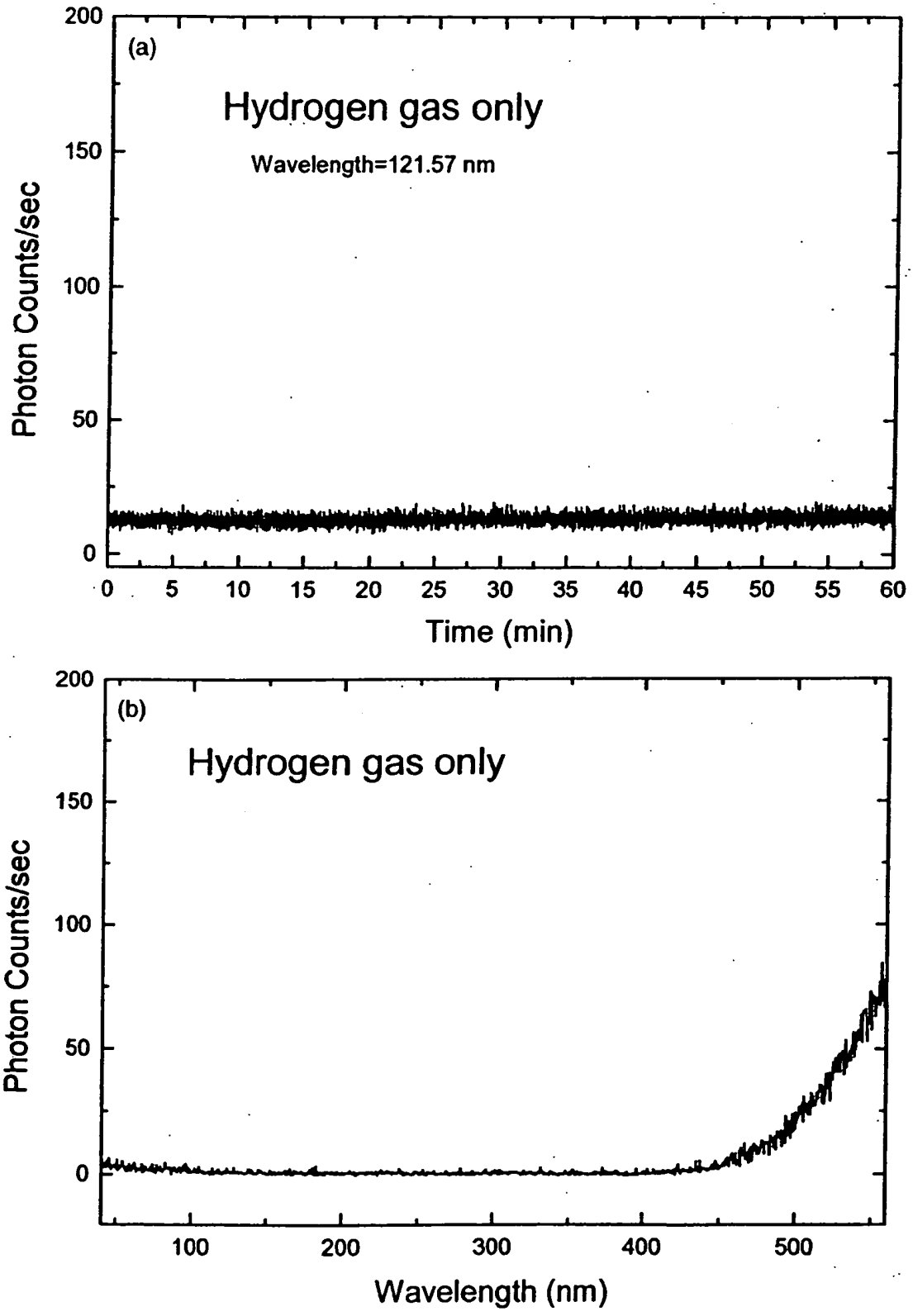

ig. 2. (*Caption overleaf*).

The intensity of the Lyman α emission as a function of time from the gas cell comprising a tungsten filament, a titanium dissociator, cesium metal versus sodium metal in the catalyst reservoir, and 0.3 torr hydrogen at a cell temperature of 700°C are shown in Fig. 3 (A) and Fig. 4, respectively. Cesium metal or sodium metal was volatized from the catalyst reservoir by heating it with an external heater. Intense emission was observed from cesium metal starting after 35 min when the cell temperature rose from room temperature to approximately 700°C. The EUV spectrum (40–160 nm) of the cell emission recorded at about the point of the maximum Lyman α emission is shown in Fig. 3(B). In the case of the sodium metal, no emission was observed. The maximum filament power was 500 W. A metal coating formed in the cap of the cell over the course of the experiment in both cases.

The intensity of the Lyman α emission as a function of time from the gas cell comprising a tungsten filament, a titanium dissociator, strontium metal in the catalyst reservoir versus a magnesium foil in the cell, and 0.3 torr hydrogen at a cell temperature of 700°C are shown in Fig. 5 (A) and Fig. 6, respectively. Strontium metal was volatized from the catalyst reservoir by heating it with an external heater. The magnesium foil was volatilized by suspending a 2 cm by 2 cm by 0.1 cm thick foil between the filament and the titanium dissociator and heating the foil with the filament. Strong emission was observed from strontium. The EUV spectrum (40–160 nm) of the cell emission recorded at about the point of the maximum Lyman α emission is shown in Fig. 5 (B). In the case of the magnesium foil, no emission was observed. The maximum filament power was 500 W. The temperature of the foil increased with filament power. At 500 W, the temperature of the foil was 1000°C which would correspond to a vapor pressure of about 100 mtorr. A magnesium metal coating formed in the cap of the cell over the course of the experiment.

The intensity of the Lyman α emission as a function of time from the gas cell comprising a tungsten filament, a titanium dissociator treated with 0.6 M K_2CO_3/10% H_2O_2 before being used in the cell, and 0.3 torr hydrogen at a cell temperature of 700°C is shown in Fig. 7. The emission reached a maximum of 60,000 counts per second at a filament power of 300 W. At this power level, potassium metal was observed to condense on the wall of the top of the gas cell. The EUV spectrum (40–160 nm) of the cell emission recorded at about the point of the maximum Lyman α emission is shown in Fig. 8 (A). The UV–VIS spectrum (40–560 nm) of the cell emission recorded with a photomultiplier tube (PMT) and a sodium salicylate scintillator from the gas cell comprising a tungsten filament, a titanium dissociator treated with 0.6 M K_2CO_3/10% H_2O_2 before being used in the cell, and 0.3 torr hydrogen at a cell temperature of 700°C is shown in Fig. 8(B). The visible spectrum is dominated by potassium lines. Hydrogen Balmer lines are also present in the UV–VIS region when the Lyman α emission is present in the EUV region. Thus, recording the Balmer emission corresponds to recording the Lyman α emission. The EUV spectrum (40–160 nm) of the cell emission recorded at about the point of the maximum Lyman α emission from the gas cell comprising a tungsten filament, a titanium dissociator treated with 0.6 M Na_2CO_3/10% H_2O_2 before being used in the cell, and 0.3 torr hydrogen at a cell temperature of 700°C is shown in Fig. 9. Essentially no emission was observed. Sodium metal was observed to condense on the wall of the top of the gas cell after the cell reached 700°C.

The results of the EUV light emission from atomic hydrogen and gaseous inorganic compounds at low temperatures (e.g. $< 10^3$ K) are summarized in Table 2. Among the inorganic compounds tested, very strong hydrogen Lyman alpha line emissions were observed from $Ba(NO_3)_2$, $RbNO_3$, $NaNO_3$, K_2CO_3, $KHCO_3$, Rb_2CO_3, Cs_2CO_3, $SrCO_3$, and $Sr(NO_3)_2$. Fig. 8(A) shows a typical EUV emission spectrum obtained by heating K_2CO_3 coated on the titanium screen in presence of atomic hydrogen. The main spectral lines were identified as atomic hydrogen Lyman alpha (121.57 nm) and Lyman beta (102.57 nm) lines, and molecular hydrogen emission lines distributed in the region 80–150 nm. The potassium ionic lines (60.07 nm, 60.80 nm and 61.27 nm) were also observed in the spectrum, but they were not resolved. The spectra show that potassium ions were formed in the cell under the experimental conditions. Their actual intensity should be larger than the observed intensity because of the lower monochromator grating efficiency at shorter wavelength.

The results of the EUV light emission from atomic hydrogen and atomized pure elements at low temperatures (e.g. $< 10^3$ K) are summarized in Table 2. Strong hydrogen Lyman alpha line emission was observed from Sr, Rb, Cs, Ca, Fe, and K.

The light emission usually occurred after the power of the filament was increased to above 300 W for about 20 min, and the light was emitted for a period

Fig. 2. (A). The intensity of the Lyman α emission as a function of time from the gas cell comprising a tungsten filament, a titanium dissociator, and 0.3 torr hydrogen at a cell temperature of 700°C. (B). The UV–VIS spectrum (40–560 nm) of the cell emission from the gas cell comprising a tungsten filament, a titanium dissociator, and 0.3 torr hydrogen at a cell temperature of 700°C that was recorded with a photomultiplier tube (PMT) and a sodium salicylate scintillator.

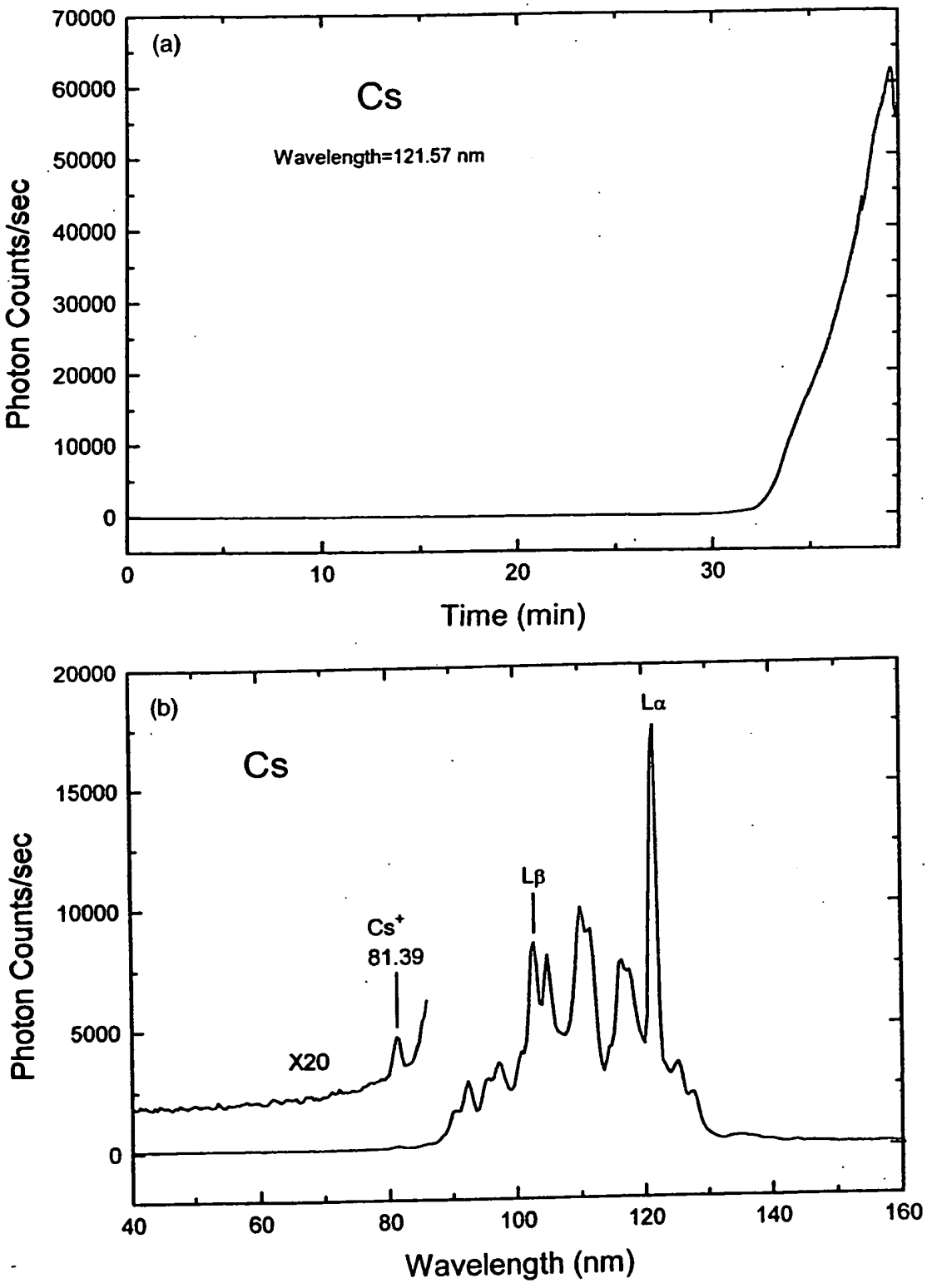

Fig. 3. (*Caption overleaf*).

depending on the temperature (heater power level), type and quantity of chemicals deposited in the cell. Higher power would cause higher temperature and higher emission intensity, but in the case of volatile chemicals, a shorter duration of emission was observed because the chemicals thermally migrated from the cell and condensed on the wall of the top of the cell. The appearance of a coating from this migration was noted in Table 2. The emission lasted from 1 h to 1 week depending on how much chemical was initially present in the cell and the power level which corresponded to the cell temperature.

4. Discussion

In the cases where Lyman α emission was observed, no possible chemical reactions of the tungsten filament, the dissociator, the vaporized test material, and 0.3 torr hydrogen at a cell temperature of 700°C could be found which accounted for the hydrogen α line emission. In fact, no known chemical reaction releases enough energy to excite Lyman α emission from hydrogen. In many cases such as the reduction of K_2CO_3 by hydrogen, any possible reaction is very endothermic. The emission was not observed with hydrogen alone or with helium, neon, or argon gas. The emission was not due to the presence of a particular anion. Ba is a very efficient source of electrons, and is commonly used to coat the cathode of a plasma discharge cell to improve the emission current [10,11]. No emission was observed with the titanium dissociator with Ba. Intense emission was observed for $NaNO_3$ with hydrogen gas, but no emission was observed when hydrogen was replaced by helium. Intense emission was observed for potassium metal with hydrogen gas, but no emission was observed when hydrogen was replaced by argon. These latter two results indicate that the emission was due to a reaction of hydrogen. The emission of the Lyman lines is assigned to the catalysis of hydrogen which excites atomic and molecular hydrogen.

The only pure elements that were observed to emit EUV are each a catalytic system wherein the ionization of t electrons from an atom to a continuum energy level is such that the sum of the ionization energies of the t electrons is approximately $m \cdot 27.2$ eV where t and m are each an integer. These elements with the specific enthalpies of the catalytic reactions appear in with the exception of neodymium metal since ionization data is unavailable.

Representative catalytic reactions appear in the balance equations *infra*. In the case that ordinary atomic hydrogen is the reactant, the parameter p which corresponds to Eq. (2) is one.

4.1. Strontium

One such catalytic system involves strontium. The first through the fifth ionization energies of strontium are 5.69484 eV, 11.03013 eV, 42.89 eV, 57 eV, and 71.6 eV, respectively [9]. The ionization reaction of Sr to Sr^{5+}, ($t = 5$), then, has a net enthalpy of reaction of 188.2 eV, which is equivalent to $m = 7$ in Eq. (3).

$$188.2\ \text{eV} + \text{Sr}(m) + \text{H}\left[\frac{a_H}{p}\right] \rightarrow \text{Sr}^{5+} + 5e^- + \text{H}\left[\frac{a_H}{(p+7)}\right] + [(p+7)^2 - p^2] \times 13.6\ \text{eV} \quad (9)$$

$$\text{Sr}^{5+} + 5e^- \rightarrow \text{Sr}(m) + 188.2\ \text{eV} \quad (10)$$

And, the overall reaction is

$$\text{H}\left[\frac{a_H}{p}\right] \rightarrow \text{H}\left[\frac{a_H}{(p+7)}\right] + [(p+7)^2 - p^2] \times 13.6\ \text{eV} \quad (11)$$

4.2. Praseodymium and neodymium metal

Another such catalytic system involves praseodymium metal. The first, second, third, fourth, and fifth ionization energies of praseodymium are 5.464 eV, 10.55 eV, 21.624 eV, 38.98 eV, and 57.53 eV, respectively [9]. The ionization reaction of Pr to Pr^{5+}, ($t = 5$), then, has a net enthalpy of reaction of 134.148 eV, which is equivalent to $m = 5$ in Eq. (3).

$$134.148\ \text{eV} + \text{Pr}(m) + \text{H}\left[\frac{a_H}{p}\right] \rightarrow \text{Pr}^{5+} + 5e^- + \text{H}\left[\frac{a_H}{(p+5)}\right] + [(p+5)^2 - p^2] \times 13.6\ \text{eV} \quad (12)$$

$$\text{Pr}^{5+} + 5e^- \rightarrow \text{Pr}(m) + 134.148\ \text{eV} \quad (13)$$

And, the overall reaction is

Fig. 3. (A). The intensity of the Lyman α emission as a function of time from the gas cell comprising a tungsten filament, a titanium dissociator, cesium metal vaporized from the catalyst reservoir, and 0.3 torr hydrogen at a cell temperature of 700°C. (B). The EUV spectrum (40–160 nm) of the cell emission recorded at about the point of the maximum Lyman α emission from the gas cell comprising cesium metal vaporized from the catalyst reservoir, a tungsten filament, a titanium dissociator, and 0.3 torr hydrogen at a cell temperature of 700°C.

$$H\left[\frac{a_H}{p}\right] \rightarrow H\left[\frac{a_H}{(p+5)}\right] + [(p+5)^2 - p^2] \times 13.6\ eV \quad (14)$$

$$\frac{134.148\ eV}{5 \times 27.196\ eV} = \frac{134.148\ eV}{135.98\ eV} = 0.987$$

EUV emission was observed in the case of praseodymium metal (Pr(m)). The count rate was about 3000 counts/second. EUV emission was also observed in the case of neodymium metal (Nd(m)). The count rate was about the same as that of praseodymium metal, 3000 counts/second. Neodymium metal (Nd(m)) may comprise a catalytic system by the ionization of 5 electrons from each neodymium atom to a continuum energy level such that the sum of the ionization energies of the 5 electrons is approximately 5·27.2 eV. The first, second, third, and fourth ionization energies of neodymium are 5.5250 eV, 10.73 eV, 21.1 eV, and 40.41 eV, respectively [9]. The fifth ionization energy of neodymium should be about that of praseodymium, 57.53 eV, based on the close match of the first four ionization energies with the corresponding ionization energies of praseodymium. In this case, the ionization reaction of Nd to Nd^{5+}, ($t = 5$), then, has a net enthalpy of reaction of 136.295 eV, which is equivalent to $m = 5$ in Eq. (3). The reaction is given by Eqs. (12)–(14) with the substitution of neodymium for praseodymium.

$$\frac{136.295\ eV}{5 \times 27.196\ eV} = \frac{136.295\ eV}{135.98\ eV} = 1.002$$

Furthermore, several cases of inorganic compounds were observed to emit EUV. The only ions that were observed to emit EUV are each a catalytic system wherein the ionization of t electrons from an ion to a continuum energy level is such that the sum of the ionization energies of the t electrons is approximately $m \cdot 27.2$ eV where m and t are each an integer. These ions with the specific enthalpies of the catalytic reactions appear in Table 1 with the exception of Ba^{2+} since ionization data is unavailable.

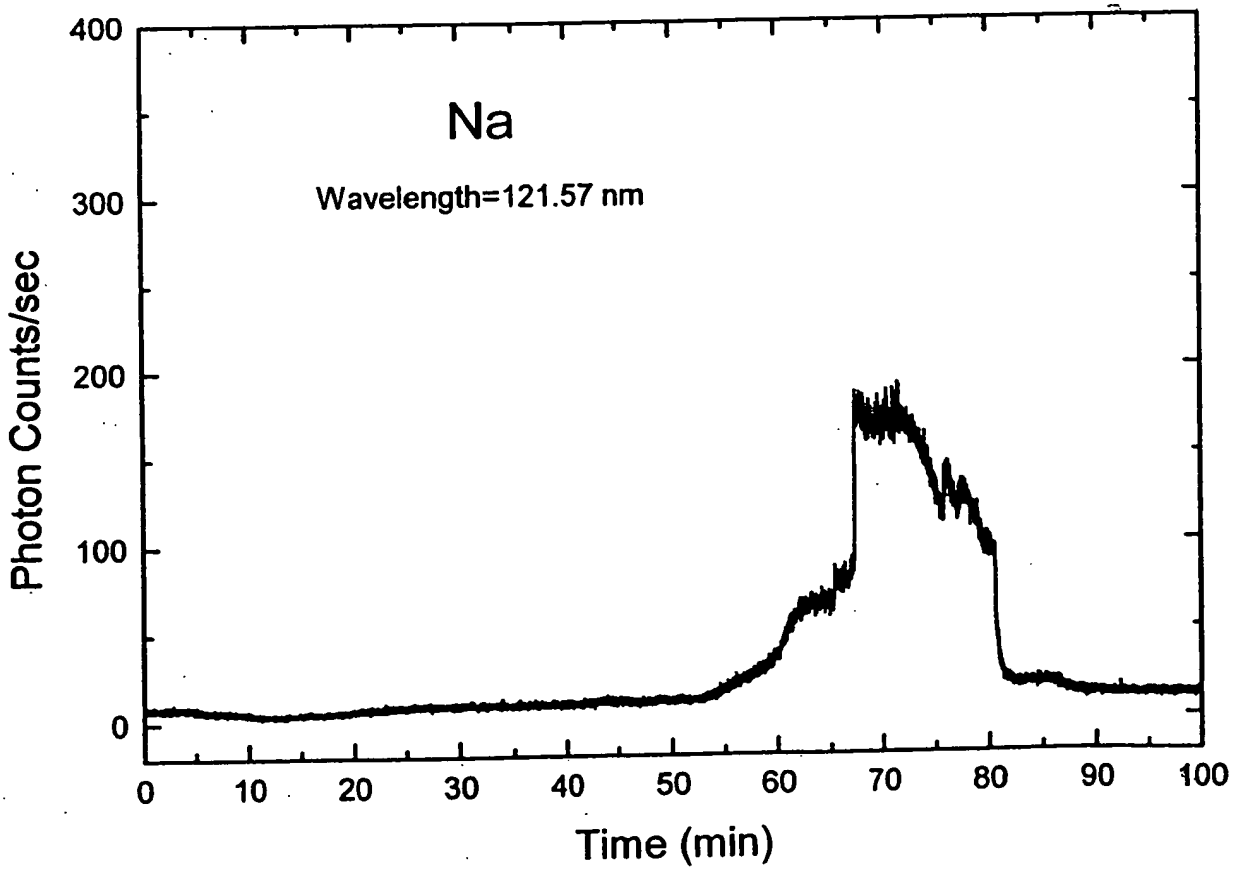

Fig. 4. The intensity of the Lyman α emission as a function of time from the gas cell comprising a tungsten filament, a titanium dissociator, sodium metal vaporized from the catalyst reservoir, and 0.3 torr hydrogen at a cell temperature of 700°C.

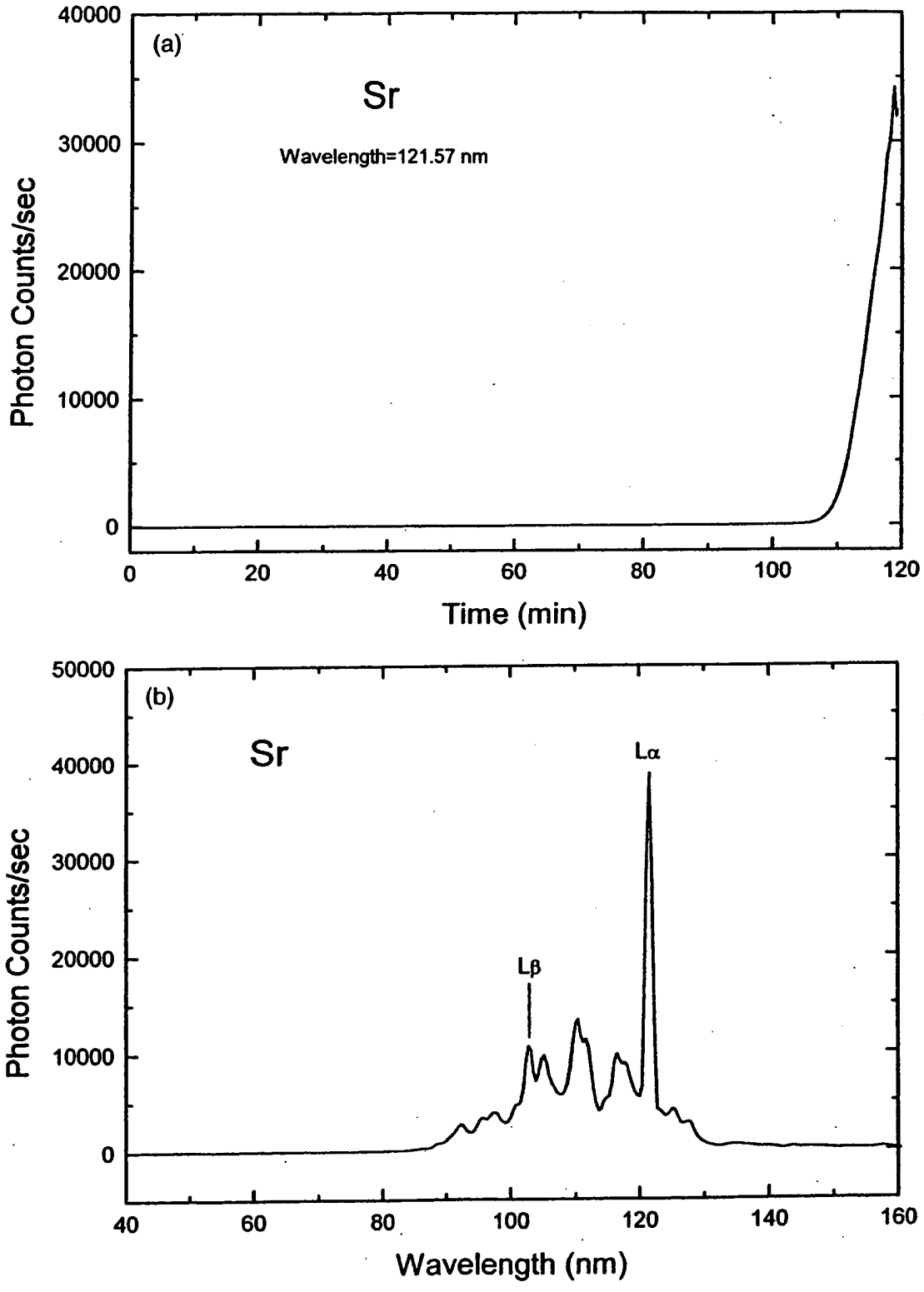

Fig. 5. (*Caption opposite*).

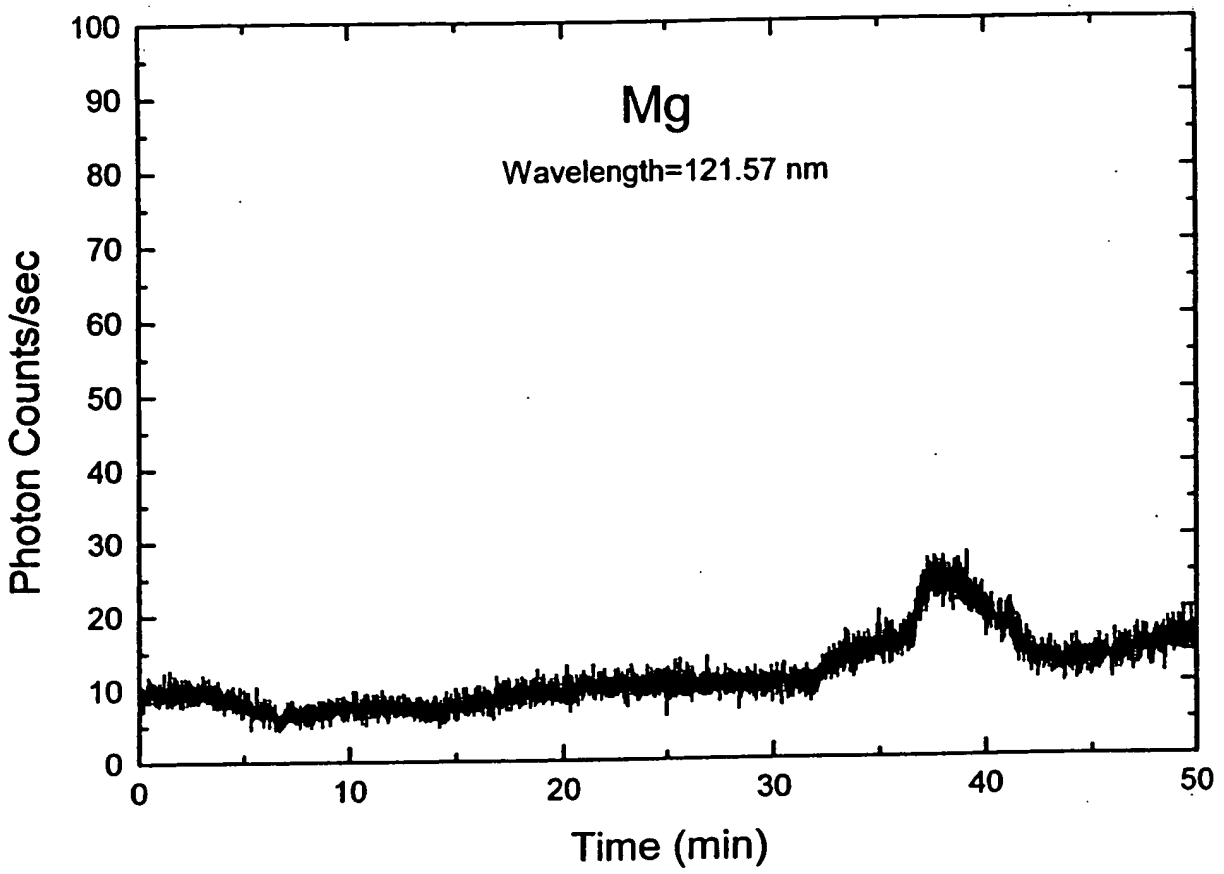

Fig. 6. The intensity of the Lyman α emission as a function of time from the gas cell comprising a tungsten filament, a titanium dissociator, a magnesium foil, and 0.3 torr hydrogen at a cell temperature of 700°C.

4.3. Rubidium

Rubidium ions can also provide a net enthalpy of a multiple of that of the potential energy of the hydrogen atom. The second ionization energy of rubidium is 27.28 eV. The reaction Rb^+ to Rb^{2+} has a net enthalpy of reaction of 27.28 eV, which is equivalent to $m = 1$ in Eq. (3).

$$27.28\,\text{eV} + Rb^+ + H\left[\frac{a_H}{p}\right] \rightarrow Rb^{2+} + e^- + H\left[\frac{a_H}{(p+1)}\right] + [(p+1)^2 - p^2] \times 13.6\,\text{eV} \quad (15)$$

$$Rb^{2+} + e^- \rightarrow Rb^+ + 27.28\,\text{eV} \quad (16)$$

The overall reaction is

$$H\left[\frac{a_H}{p}\right] \rightarrow H\left[\frac{a_H}{(p+1)}\right] + [(p+1)^2 - p^2] \times 13.6\,\text{eV} \quad (17)$$

The catalytic rate and corresponding intensity of EUV emission depends of the concentration of gas phase Rb^+ ions. Rubidium metal may form RbH which may provide gas phase Rb^+ ions, or rubidium metal may be ionized to provide gas phase Rb^+ ions. Rb_2CO_3 comprises two Rb^+ ions rather than one, and it is not as volatile. But, it may decompose to rubidium metal

Fig. 5. (A). The intensity of the Lyman α emission as a function of time from the gas cell comprising a tungsten filament, a titanium dissociator, strontium metal vaporized from the catalyst reservoir, and 0.3 torr hydrogen at a cell temperature of 700°C. (B). The EUV spectrum (40–160 nm) of the cell emission recorded at about the point of the maximum Lyman α emission from the gas cell comprising a tungsten filament, a titanium dissociator, strontium metal vaporized from the catalyst reservoir, and 0.3 torr hydrogen at a cell temperature of 700°C.

in which case the vapor pressure should be higher than that vaporized from the catalyst reservoir due to the large surface area of the rubidium coated titanium dissociator. Alkali metal nitrates are extraordinarily volatile and can be distilled at 350–500°C [12]. $RbNO_3$ is the favored candidate for providing gaseous Rb^+ ions. The EUV spectrum (40–160 nm) of the cell emission recorded at about the point of the maximum Lyman α emission for rubidium metal, Rb_2CO_3, and $RbNO_3$ is shown in Fig. 10. $RbNO_3$ produced the highest intensity EUV emission.

4.4. Sodium iodide, sodium metal, sodium carbonate, sodium nitrate

No emission was observed in the case of NaI. No emission was observed in the case of KI either which indicates that iodides form a molecular bond in the gas phase. Essentially no EUV emission was observed in the case of Na(m) and Na_2CO_3. What little was observed may be due to potassium contamination which was measured by time-of-flight-secondary-ion-mass-spectroscopy. EUV emission was observed in the case of $NaNO_3$. Na(m) is not a catalyst. Na_2CO_3 decomposes to Na(m). Na_2CO_3 is further not a catalyst because two sodium ions are present rather than one, and Na_2CO_3 is not volatile. $NaNO_3$ is a catalyst which is volatile at the experimental conditions of the EUV experiment. The catalytic system is provided by the ionization of three electrons from Na^+ to a continuum energy level such that the sum of the ionization energies of the three electrons is approximately m·27.2 eV where m is an integer. The second, third, and fourth ionization energies of sodium are 47.2864 eV, 71.6200 eV, and 98.91 eV, respectively [9]. The triple ionization reaction of Na^+ to Na^{4+}, then, has a net enthalpy of reaction of 217.8164 eV, which is equivalent to $m = 8$ in Eq. (3).

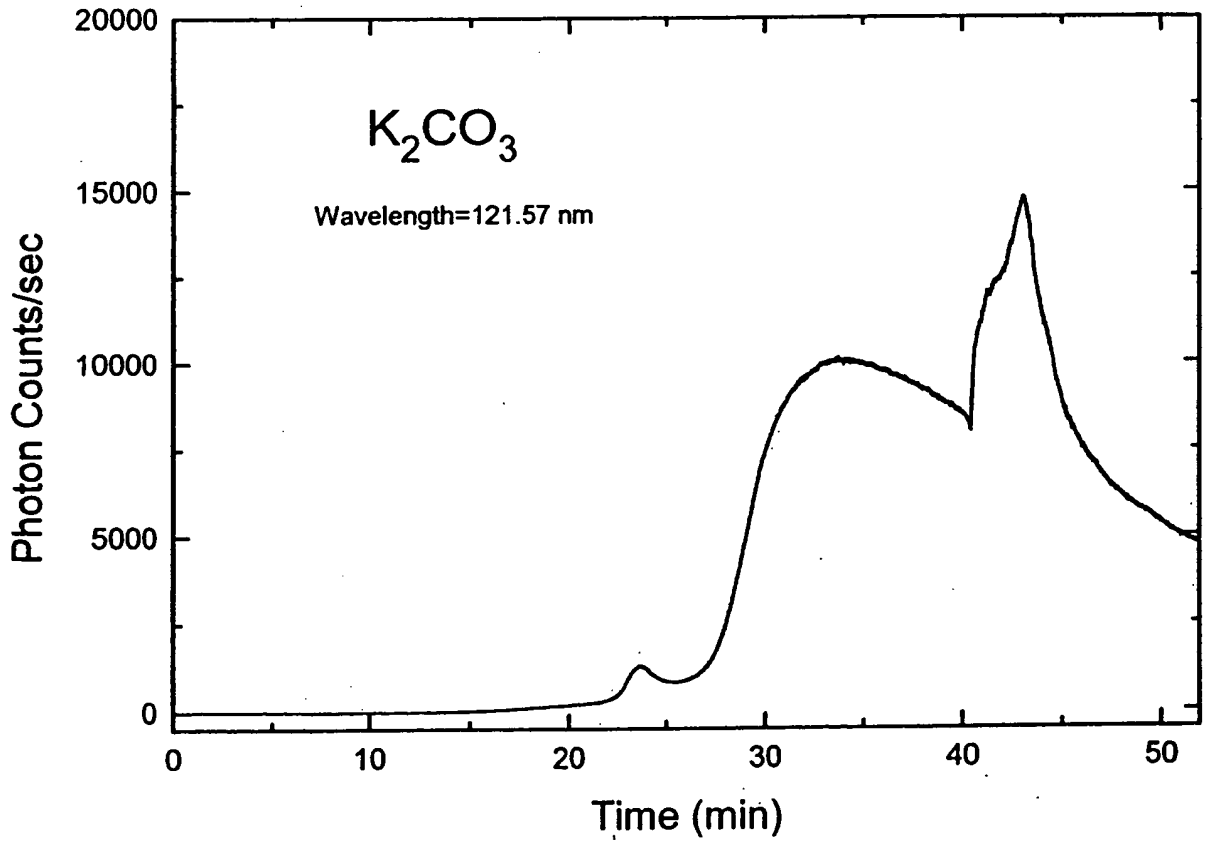

Fig. 7. The intensity of the Lyman α emission as a function of time from the gas cell comprising a tungsten filament, a titanium dissociator treated with 0.6 M K_2CO_3/10% H_2O_2 before being used in the cell, and 0.3 torr hydrogen at a cell temperature of 700°C.

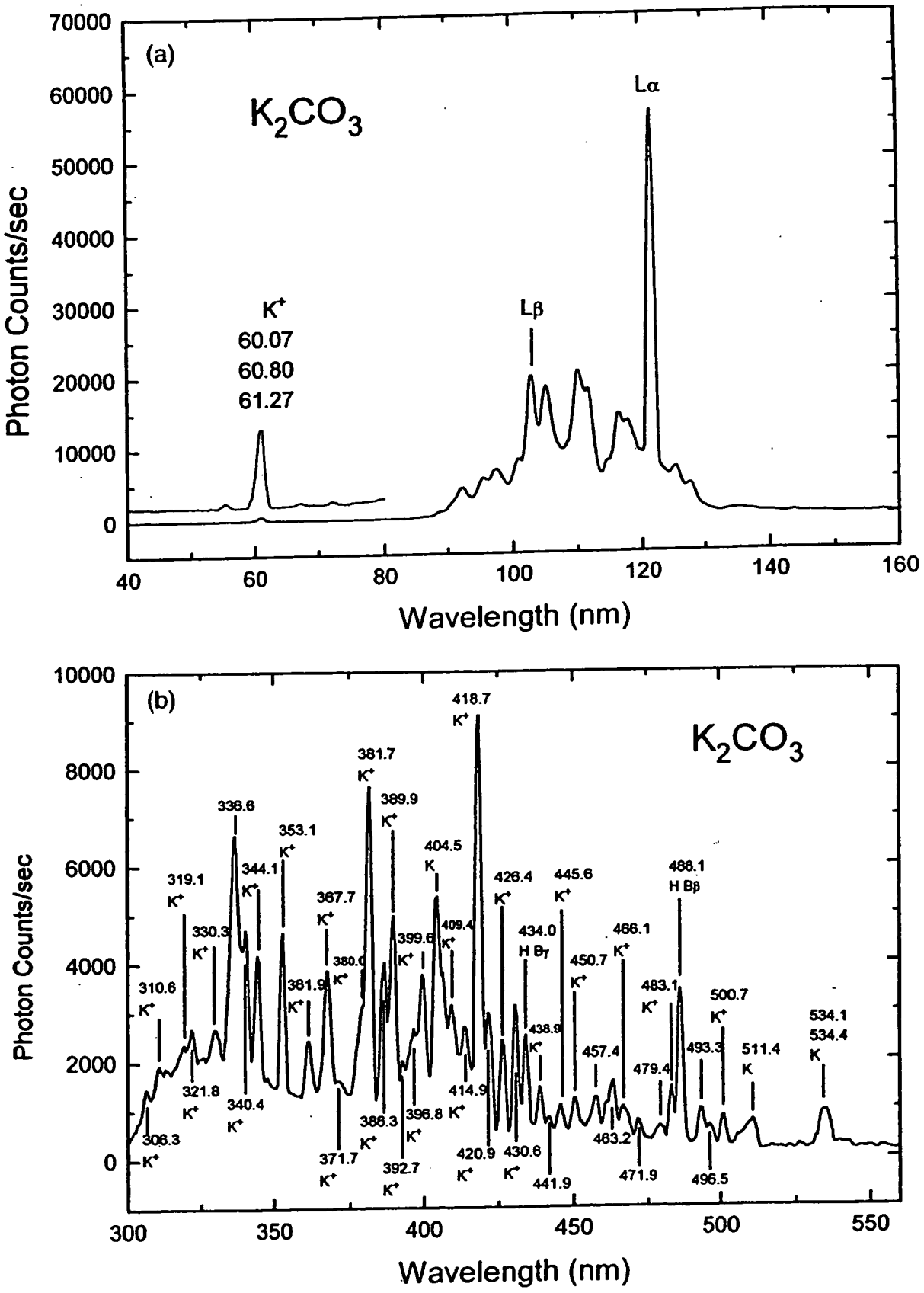

Fig. 8. (Caption overleaf).

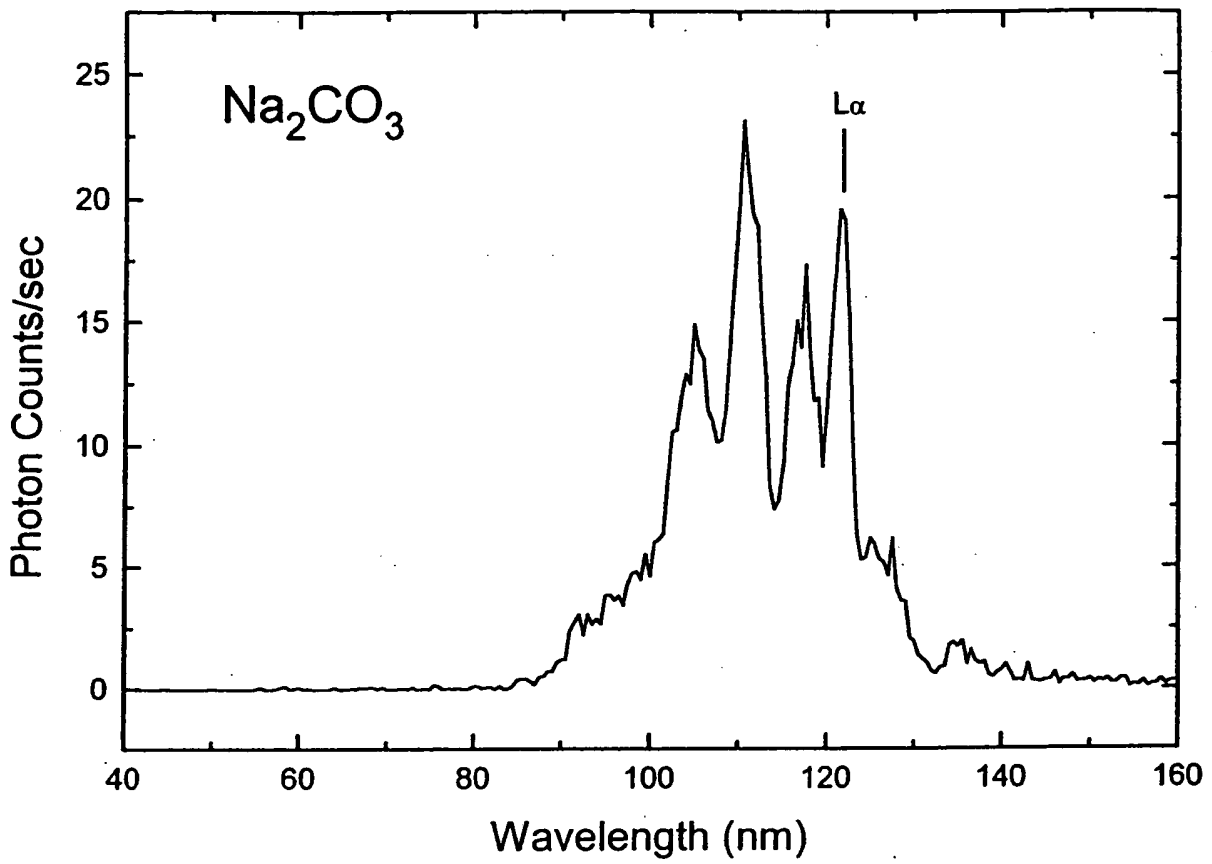

Fig. 9. The EUV spectrum (40–160 nm) of the cell emission recorded at about the point of the maximum Lyman α emission from the gas cell comprising a tungsten filament, a titanium dissociator treated with 0.6 M Na_2CO_3/10% H_2O_2 before being used in the cell, and 0.3 torr hydrogen at a cell temperature of 700°C.

$$217.8164\ \text{eV} + Na^+ + H\left[\frac{a_H}{p}\right] \rightarrow Na^{4+} + 3e^- + H\left[\frac{a_H}{(p+8)}\right] + [(p+8)^2 - p^2] \times 13.6\ \text{eV} \quad (18)$$

$$Na^{4+} + 3e^- \rightarrow Na^+ + 217.8164\ \text{eV} \quad (19)$$

And, the overall reaction is

$$H\left[\frac{a_H}{p}\right] \rightarrow H\left[\frac{a_H}{(p+8)}\right] + [(p+8)^2 - p^2] \times 13.6\ \text{eV} \quad (20)$$

$$\frac{217.8164\ \text{eV}}{8 \times 27.196\ \text{eV}} = \frac{217.8164\ \text{eV}}{217.568\ \text{eV}} = 1.001$$

Very little mirroring was observed compared to that observed with the onset of EUV emission in the case of K_2CO_3 or KNO_3. This further supports the source of emission as $NaNO_3$ catalyst.

Fig. 8. (A). The EUV spectrum (40–160 nm) of the cell emission recorded at about the point of the maximum Lyman α emission from the gas cell comprising a tungsten filament, a titanium dissociator treated with 0.6 M K_2CO_3/10% H_2O_2 before being used in the cell, and 0.3 torr hydrogen at a cell temperature of 700°C. (B). The UV–VIS spectrum (300–560 nm) of the cell emission recorded with a photomultiplier tube (PMT) and a sodium salicylate-scintillator from the gas cell comprising a tungsten filament, a titanium dissociator treated with 0.6 M K_2CO_3/10% H_2O_2 before being used in the cell, and 0.3 torr hydrogen at a cell temperature of 700°C.

4.5. Barium nitrate

EUV emission was observed from $Ba(NO_3)_2$; whereas, no EUV emission was observed from Ba(m). Alkali metal nitrates are extraordinarily volatile and can be distilled 350–500°C, and barium nitrate can also be distilled at 600°C [12]. $Ba(NO_3)_2$ melts at 592°C; thus, it is stable and volatile at the operating temperature of the EUV experiment. Ba^{2+} may be a catalyst, but it is not possible to determine this since only the first two vacuum ionization energies of barium are published [9].

A catalysts may also be provided by the transfer of t electrons between participating ions. The transfer of t electrons from one ion to another ion provides a net enthalpy of reaction whereby the sum of the ionization energy of the electron donating ion minus the ionization energy of the electron accepting ion equals approximately $m \cdot 27.2$ eV where t and m are each an integer. Two K^+ ions in one case and two La^{3+} ions in another were observed to serve as catalysts as indicated by the observed EUV emission. No other ion pairs caused EUV emission.

4.6. Potassium

Potassium ions can also provide a net enthalpy of a multiple of that of the potential energy of the hydrogen atom. The second ionization energy of potassium is 31.63 eV; and K^+ releases 4.34 eV when it is reduced to K. The combination of reactions K^+ to K^{2+} and K^+ to K, then, has a net enthalpy of reaction of 27.28 eV, which is equivalent to $m = 1$ in Eq. (3).

$$27.28\ \text{eV} + K^+ + K^+ + H\left[\frac{a_H}{p}\right] \rightarrow K + K^{2+} + H\left[\frac{a_H}{(p+1)}\right] + [(p+1)^2 - p^2] \times 13.6\ \text{eV} \quad (21)$$

$$K + K^{2+} \rightarrow K^+ + K^+ + 27.28\ \text{eV} \quad (22)$$

The overall reaction is

$$H\left[\frac{a_H}{p}\right] \rightarrow H\left[\frac{a_H}{(p+1)}\right] + [(p+1)^2 - p^2] \times 13.6\ \text{eV} \quad (23)$$

4.7. Lanthanum carbonate

EUV emission was observed from $La_2(CO_3)_3$; whereas, no emission was observed from lanthanum metal or $La(NO_3)_3$. Lanthanum metal is not a catalyst. A single La^{3+} corresponding to the case of $La(NO_3)_3$ is also not a catalyst. In another embodiment, a catalytic system transfers two electrons from one ion to another such that the sum of the total ionization energy of the electron donating species minus the total ionization energy of the electron accepting species equals approximately $m \cdot 27.2$ eV where m is an integer. One such catalytic system involves lanthanum as $La_2(CO_3)_3$ which provides two La^{3+} ions. The only stable oxidation state of lanthanum is La^{3+}. The fourth and fifth ionization energies of lanthanum are 49.95 eV and 61.6 eV, respectively. The third and second ionization energies of lanthanum are 19.1773 eV and 11.060 eV, respectively [9]. The combination of reactions La^{3+} to La^{5+} and La^{3+} to La^+, then, has a net enthalpy of reaction of 81.3127 eV, which is equivalent to $m = 3$ in Eq. (3).

$$81.3127\ \text{eV} + La^{3+} + La^{3+} + H\left[\frac{a_H}{p}\right] \rightarrow La^{5+} + La^+ + H\left[\frac{a_H}{(p+3)}\right] + [(p+3)^2 - p^2] \times 13.6\ \text{eV} \quad (24)$$

$$La^{5+} + La^+ \rightarrow La^{3+} + La^{3+} + 81.3127\ \text{eV} \quad (25)$$

The overall reaction is

$$H\left[\frac{a_H}{p}\right] \rightarrow H\left[\frac{a_H}{(p+3)}\right] + [(p+3)^2 - p^2] \times 13.6\ \text{eV} \quad (26)$$

$$\frac{81.3127\ \text{eV}}{3 \times 27.196\ \text{eV}} = \frac{81.3127\ \text{eV}}{81.588\ \text{eV}} = 0.997$$

4.8. Germanium

Weak (100 counts/sec) EUV emission was observed from Ge. The stable oxidation states of germanium are Ge^{2+} and Ge^{4+}. The catalytic system is provided by the ionization of two electrons from Ge^{2+} to a continuum energy level such that the sum of the ionization energies of the two electrons is approximately $m \cdot 27.2$ eV where m is an integer. The third and fourth ionization energies of germanium are 34.2241 eV, and 45.7131 eV, respectively [9]. The double ionization reaction of Ge^{2+} to Ge^{4+}, then, has a net enthalpy of reaction of 79.9372 eV, which is equivalent to $m = 3$ in Eq. (3).

$$79.9372\ \text{eV} + Ge^{2+} + H\left[\frac{a_H}{p}\right] \rightarrow Ge^{4+} + 2e^- + H\left[\frac{a_H}{(p+3)}\right] + [(p+3)^2 - p^2] \times 13.6\ \text{eV} \quad (27)$$

$$Ge^{4+} + 2e^- \rightarrow Ge^{2+} + 79.9372\ \text{eV} \quad (28)$$

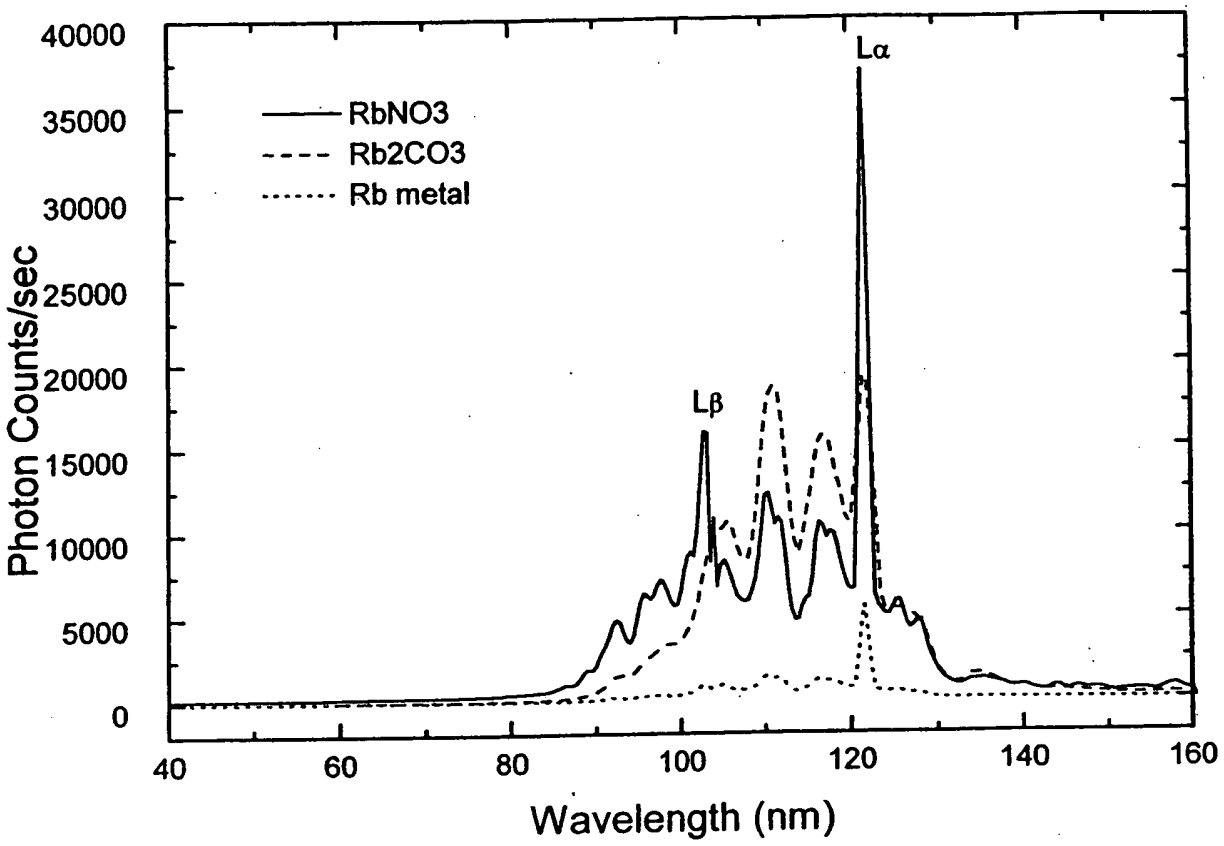

Fig. 10. The EUV spectrum (40–160 nm) of the cell emission recorded at about the point of the maximum Lyman α emission from the gas cell comprising rubidium metal, Rb_2CO_3, or $RbNO_3$, a tungsten filament, a titanium dissociator, and 0.3 torr hydrogen at a cell temperature of 700°C.

And, the overall reaction is

$$H\left[\frac{a_H}{p}\right] \rightarrow H\left[\frac{a_H}{(p+3)}\right] + [(p+3)^2 - p^2] \times 13.6\,eV \quad (29)$$

$$\frac{79.9372\,eV}{3 \times 27.196\,eV} = \frac{79.9372\,eV}{81.588\,eV} = 0.98$$

Very low level EUV emission with the presence of some of the elements in Table 1 may be explained by the presence of low levels of catalytic ions of a pure element such as the case of germanium or by contamination with catalytic reactants such as potassium in sodium.

5. Conclusions

Intense EUV emission was observed at low temperatures (e.g. $< 10^3$ K) from atomic hydrogen and certain atomized pure elements or certain gaseous ions which ionize at integer multiples of the potential energy of atomic hydrogen. The release of energy from hydrogen as evidenced by the EUV emission must result in a lower-energy state of hydrogen. The lower-energy hydrogen atom called a hydrino atom by Mills [6] would be expected to demonstrate novel chemistry. The formation of novel compounds based on hydrino atoms would be substantial evidence supporting catalysis of hydrogen as the mechanism of the observed EUV emission. A novel hydride ion called a hydrino hydride ion having extraordinary chemical properties given by Mills [6] is predicted to form by the reaction of an electron with a hydrino atom. Compounds containing hydrino hydride ions have been isolated as products of the reaction of atomic hydrogen with atoms and ions identified as catalysts in the present EUV study [6,13,14]. Work is in progress to optimize the EUV emission and correlate the EUV emission with novel compound and heat production.

Billions of dollars have been spent to harness the energy of hydrogen through fusion using plasmas created and heated to extreme temperatures by RF coupling (e.g. $> 10^6$ K) with confinement provided by a

toroidal magnetic field. The present study indicates that energy may be released from hydrogen at relatively low temperatures with an apparatus which is of trivial technological complexity compared to a tokomak. And, rather than producing radioactive waste, the reaction has the potential to produce compounds having extraordinary properties. The implications are that a vast new energy source and a new field of hydrogen chemistry have been discovered.

Acknowledgements

Special thanks to Nelson Greenig for designing the fiber optic system, to Grace Christ for preparing many of the cells comprising the test materials, and to Jiliang He for reviewing this manuscript.

References

[1] Phillips JH. In: Guide to the Sun. Cambridge, UK: Cambridge University Press, 1992. p. 16–20.
[2] Sampson JAR, Techniques of vacuum ultraviolet spectroscopy, Pied Publications, 1980, 94–179.
[3] Science News, 12/6/97, 366.
[4] Fujimoto T, Sawada K, Takahata K. J Appl Phys 1989;66(6):2315–9.
[5] Hollander A, Wertheimer MR. J Vac Sci Technol A 1994;12(3):879–82.
[6] Mills R. The Grand unified theory of classical quantum mechanics. January 1999 Edition. Cranbury, New Jersey: BlackLight Power, 1999 Distributed by Amazon.com.
[7] Sidgwick NV. In: The chemical elements and their compounds, vol. I. Oxford: Clarendon Press, 1950. p. 17.
[8] Lamb MD. In: Luminescence spectroscopy. London: Academic Press, 1978. p. 68.
[9] David R Linde. In: CRC handbook of chemistry and physics. 79th Ed. Boca Raton, Florida: CRC Press, 1998-9. p. 10,175–10,1777.
[10] Sampson, JAR, Techniques of vacuum ultraviolet spectroscopy, Pied Publications, (1980), 147.
[11] M. Benjamin, The London, Edinburgh, and Dublin, Philosophical Magazine and Journal of Science 1935:July; 1–24.
[12] C.J. Hardy, B.O. Field, J. Chem. Soc. 1963;5130–5134.
[13] Mills R., Dhandapani B., Greenig N., He J, Synthesis and characterization of potassium iodo Hydride, Int. J. of Hydrogen Energy in Progress.
[14] Mills R., Novel hydride compound, Int. J. of Hydrogen Energy, accepted.